Beliaev damping of quasi-particles in a Bose-Einstein condensate

N. Katz, J. Steinhauer, R. Ozeri, and N. Davidson
Department of Physics of Complex Systems,
Weizmann Institute of Science, Rehovot 76100, Israel

We report a measurement of the suppression of collisions of quasi-particles with ground state atoms within a Bose-Einstein condensate at low momentum. These collisions correspond to Beliaev damping of the excitations, in the previously unexplored regime of the continuous quasi-particle energy spectrum. We use a hydrodynamic simulation of the expansion dynamics, with the Beliaev damping cross-section, in order to confirm the assumptions of our analysis.

In a Bose-Einstein condensate (BEC) collisions with distinguishable excitations (impurities) and collisions with indistinguishable excitations (quasi-particles) differ profoundly. These differences follow from the quantum exchange symmetry of the indistinguishable excitations, and from a different excitation spectrum.

Impurity collisions within a BEC have been measured previously. Using Raman spectroscopy the microscopic onset of superfluidity was measured and found to be in general agreement with prediction [1]. The collisional dynamics and interaction between two distinguishable slowly moving condensates was measured [2] and found to agree with simulation [3]. Macroscopic superfluid behavior has also been demonstrated, involving the interaction of the condensate with large-scale optical dipole-potential structures [4], [5].

The case of identical particle collisions has been extensively studied using many-body theory, starting with [6]. Recently, these results have been applied to BEC explicitly [7], [8], [9], [10]. In this letter we present a measurement of collisions between quasi-particles and the BEC, at velocities near and above the superfluid critical velocity v_c.

According to the Fermi golden rule, the rate of scattering within a homogenous BEC is given by [11]:

$$n\sigma_k v_k = 2^{7/2} n a^2 v_c \int dq d\Omega q^2 \left|A_{q;k}\right|^2 \delta(E_i - E_f) \quad (1)$$

where a is the s-wave scattering length. The wavenumber k of the excitation is in units of $\xi^{-1} = \sqrt{8\pi n a}$, the inverse healing length of the condensate. The free particle velocity of the excitations is $v_k = \hbar k \xi^{-1}/m$, where m the mass of the BEC atoms. n is the density of the condensate. The superfluid critical velocity is $v_c = \sqrt{\mu/m}$, where $\mu = gn$ is the chemical potential of the BEC, and g is $4\pi\hbar^2 a/m$. The integral is over all possible momentum transfers q, and all angles Ω. The δ-function requires energy conservation between the initial energy E_i and the final energy E_f after collision, where we express energy in units of μ. The factor $A_{q;k}$ is the q-dependent, momentum conserving, scattering matrix element of an excitation of wavenumber k, which may include suppression or enhancement of the collision process due to many-body effects.

For impurity scattering within a condensate [11], $\left|A_{q;k}\right|^2$ is given by the structure factor S_q [12]. The initial energy $E_i = E_k^0$, where $E_k^0 = k^2$ is the impurity dispersion relation, for impurities with mass m. The final energy for this process is $E_f = E^0_{\mathbf{k-q}} + E_q^B$, where $E_q^B = \sqrt{q^4 + 2q^2}$ is the recently measured [13] Bogoliubov dispersion relation [14].

Below v_c collisions between the impurity and condensate are completely suppressed (see Fig. 1) by the δ-function requiring conservation of energy and momentum.

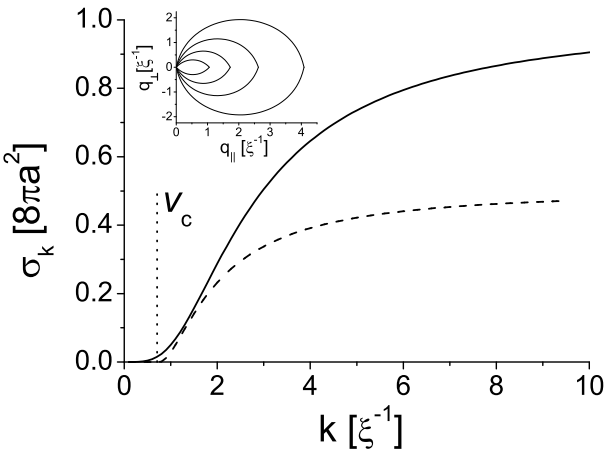

FIG. 1. Cross-section for collisions in a homogenous condensate. The momentum is in units of the inverse healing length, $\xi^{-1} = \sqrt{8\pi n a}$. The cross-section is in units of the free particle scattering cross-section for identical particles $8\pi a^2$. The solid line is the theoretical curve, from Eq. (3) for quasi-particles travelling through the condensate. The dashed line is the cross-section for impurity scattering within the condensate [1], which vanishes below the superfluid critical velocity v_c. The inset shows the allowed momentum manifold for quasi-particle collisions due to conservation of energy and momentum. The $q_\parallel$ and $q_\perp$ axes correspond to the parallel and orthogonal components of the scattered momentum respectively, where $tan(\theta) = q_\perp/q_\parallel$. The manifolds represent the experimental k's 4.09 (outermost), 2.63, 1.73 and 1.06 (innermost).

In the case of quasi-particle collisions only the Bogoliubov dispersion relation is relevant, and the δ-function in Eq. (1) is simply $\delta(E_k^B - E_q^B - E^B_{\mathbf{k-q}})$. We solve this condition, and find the angle θ between the initial direc-

tion $\mathbf{k}$ and the scattered direction $\mathbf{q}$, to be (see inset of Fig. 1):

$$\cos(\theta) = (2kq)^{-1}\left[k^2+q^2+1-\sqrt{1+(E_k^B-E_q^B)^2}\right] \tag{2}$$

This result differs in a qualitative way from impurity scattering, since Eq. (2) has solutions for any finite k. There is no longer any well-defined critical velocity at which collisions are completely suppressed. However, not all angles are allowed. At a given k we find that the maximal allowed angle is $cos(\theta_{max}) = \sqrt{(k^2+2)/2}/(k^2+1)$. At the limit of small k, this angle approaches zero, and collisions are allowed only for $\mathbf{q}$ parallel to $\mathbf{k}$.

The appropriate suppression term $|A_{q;k}|^2$ for quasi-particles has been calculated [7], [8]. In this work we expect mainly Beliaev processes which involve creation of lower energy excitations. The Landau damping rate is expected to be an order of magnitude slower than the observed Beliaev collision process [8].

We start with the atomic interaction Hamiltonian $H' = \frac{g}{2V}\sum_{j,l,m,n} a_j^\dagger a_l^\dagger a_m a_n \delta_{j+l-m-n}$, where V is the volume of the BEC, $a_i^\dagger$ and a_i are the atomic creation and annihilation operators at wavenumber i. We approximate $a_0^\dagger \approx a_0 \approx \sqrt{N_0}$, with N_0 the number of atoms in the condensate. We take the Bogoliubov transform $a_p^\dagger = (u_p b_p^\dagger - v_p b_{-p})$, with u_p and v_p the appropriate quasi-particle amplitudes, which were recently measured [15]. We are interested in terms of the form $b_k b_{\mathbf{k-q}}^\dagger b_q^\dagger$, that remove a quasi-particle of wave number k, and create two in its stead. Calculating the matrix element prefactor of this term in the atomic interaction Hamiltonian, we arrive at $A_{q;k} = \frac{1}{2}(S_q + 3S_qS_kS_{\mathbf{k-q}} + S_{\mathbf{k-q}} - S_k)/\sqrt{S_kS_qS_{\mathbf{k-q}}}$. This result can be viewed as the explicit zero temperature limit of more general calculations [10].

Applying Eq. (2) and $|A_{q;k}|^2$ to Eq. (1), and using the Feynman relation [16] $S_q = E_q^0/E_q^B$, we arrive at the rate of excitation-condensate collisions:

$$n\sigma_k^B v_k = 8\pi n a^2 v_k \times \frac{1}{2k^2}\int_0^k dqq\,|A_{q;k}|^2\,\frac{E_k^B-E_q^B}{\sqrt{1+(E_k^B-E_q^B)^2}} \tag{3}$$

The effective cross-section σ_k^B for the quasi-particles, is shown in Fig. 1 (solid line). For large k, σ_k^B approaches $8\pi a^2$, compared to $4\pi a^2$ for impurities (dashed line). This enhancement by a factor of 2 is due to the boson quantum mechanical exchange term. In Eq. (3), for small k, we verify that the scattering rate indeed scales as k^5, which is the classic result [6], [8]. In particular, it remains finite even for $v_k < v_c$, in contrast with impurity scattering.

In [1], the identical particle collision cross section for large k was measured to be $2.1(\pm 0.3)\times 4\pi a^2$. Scattering rates in four-wave mixing experiments in BEC [17] were also shown to agree with the high-k limit of Eq. (3) [18].

In the opposite regime of extremely low wavenumber, where the energy levels are discrete, Beliaev damping was observed for the scissors mode of a BEC [19]. The discrete energy levels were tuned so that Beliaev damping of the initial mode to exactly one mode of half the energy was achieved. Eq. (3) did not apply, since there was no need to integrate over various scattering modes.

Our experimental apparatus is described in [13]. Briefly, a nearly pure ($> 95\%$) BEC of 10^5 ^{87}Rb atoms in the $|F, m_f\rangle = |2,2\rangle$ ground state, is formed in a QUIC type magnetic trap [20]. The trap is cylindrically symmetric, with radial ($\hat{r}$) and axial ($\hat{z}$) trapping frequencies of $2\pi \times 220$ Hz and $2\pi \times 25$ Hz, respectively. Thus $\xi = 0.24\mu m$ via averaging in the local density approximation (LDA) [13].

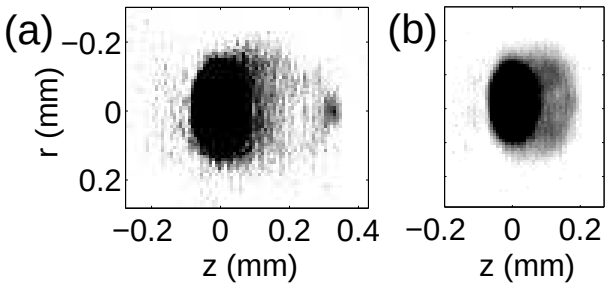

FIG. 2. Absorption TOF images of excited Bose-Einstein condensates. (a) Absorption image for $k = 2.63$, with the large cloud at the origin corresponding to the unperturbed BEC. A clear halo of scattered atoms is visible between the BEC and the cloud of unscattered outcoupled excitations. (b) Absorption image for $k = 1.06$. For this value of k the distinction between scattered and unscattered excitations is not clear, since both types of excitations occupy the same region in space.

We excite quasi-particles at a well-defined wavenumber using two-photon Bragg transitions [21]. The two Bragg beams are detuned 6.5 GHz from the $5S_{1/2}, F = 2 \longrightarrow 5P_{3/2}, F' = 3$ transition. The frequency difference $\Delta\omega$ between the two lasers is controlled via two acousto-optical modulators. Bragg pulses of 1 msec duration are applied to the condensate. The angle between the beams is varied to produce excitations of various k along the z-axis, thus preserving the cylindrical symmetry of the unperturbed BEC. The beam intensities are chosen to excite no more than 20% of the total number of atoms in the condensate.

After the Bragg pulse, the magnetic trap is rapidly turned off, and after a short acceleration period the interaction energy between the atoms is converted into ballistic kinetic energy [22]. After 38 msec of time-of-flight (TOF) expansion the atomic cloud is imaged by

an on-resonance absorption beam, perpendicular to the z-axis. Fig. 2a shows the resulting absorption image for $k = 2.63$, with the large cloud at the origin corresponding to the BEC. A halo of scattered atoms is visible between the BEC and the cloud of unscattered outcoupled excitations. No excitations with energy greater than that of the unscattered excitations are observed, confirming our low estimate of the Landau damping rate. Fig. 2b shows the absorption image for $k = 1.06$. For this k value the distinction between scattered and unscattered excitations is not clear in the image, since both types of excitations occupy the same region in space.

At a given k the number of excitations is varied by scanning $\Delta\omega$ around the resonance frequency ω_k^B. The number of excitations N_{mom} is measured by determining the total momentum (in units of the recoil momentum $\hbar k\xi^{-1}$) contained in the outcoupled region outside the unperturbed BEC. This region includes all the scattered and unscattered excitations, in the direction of $\mathbf{k}$. Thermal effects are removed by subtracting the result of an identical analysis over the other side. The results are shown in Fig. 3a.

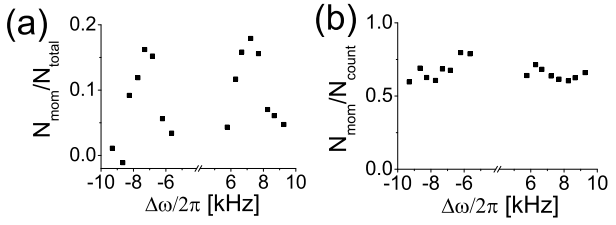

FIG. 3. Quantifying the amount of collisions measured for $k = 2.63$. (a) Measured momentum of the outcoupled atoms vs. $\Delta\omega$. The momentum is in units of the recoil momentum, and is normalized by the total number of atoms. (b) The measured ratio between N_{mom} and N_{count} (both defined in the text). Every collision outcouples more atoms, increasing N_{count} but leaving N_{mom} almost unchanged.

In order to quantify the amount of collisions, despite the lack of separation between scattered and unscattered excitations, we take the ratio between N_{mom} and the counted number of atoms N_{count}, in the same region. The resulting N_{mom}/N_{count}, as a function of $\Delta\omega$, are shown in Fig. 3b. The ratio is seen to be independent of the number of excitations, and appears to be an intrinsic property of a single excitation. Each collision between an excitation and the condensate creates an additional excitation that is counted in the outcoupled region, increasing N_{count}, while the momentum (N_{mom}) in this interaction is conserved. Thus the ratio, N_{mom}/N_{count}, is a good quantifier of the amount of the collisions, even at low k [23]. Bosonic amplification of the collision rate [11], which would appear as minima in Fig 3b, is not observed.

At a given k we define the overall probability for an excitation to undergo the first collision p_k. If we ignore secondary collisions the result is $N_{mom}/N_{count} = 1/(1+p_k)$, since each collision outcouples, after TOF, an additional particle [24]. Using this relation we infer p_k^{exp} for the various measured k's.

We expect the scattering probability p_k to be equal to $\tilde{n}\sigma_k^B v_k t_{eff}$, where t_{eff} is the effective interaction time of the excitation with condensate and $\tilde{n}$ is the average density.

We assume t_{eff} to be k-independent, divide p_k by v_k, and arrive at a value that is proportional to the scattering cross section (since the $\tilde{n}$ is constant for all k). This assumption will be tested below, but must be valid for sufficiently low k, for which the TOF expansion lowers the density rapidly, turning off collisions before the excitations move significantly.

The ratio, $p_k^{exp}/(\tilde{n}v_k t_{eff})$ is shown in Fig. 4 (■) and seen to agree with the theoretical suppression (solid line) calculated as a LDA average [12] of Eq. (3) [25]. Since t_{eff} is not known, absolute calibration is not possible. Therefore, the results are shown with arbitrary units.

In order to verify the validity of these simplifying assumptions, 3-D simulations are performed, using the hydrodynamic Gross-Pitaevskii equations [26]. The simulations [22] include the TOF dynamics. The expansion of the main BEC cloud is taken from expressions in [27], computed for an elongated condensate by the hydrodynamic equations. The excitations travel within the time varying mean field potential created by the expanding unperturbed condensate. The excitations collide with the expanding condensate with the correct local scattering cross section, including the angular dependence, taken from Eq. (3). The resulting distribution of simulated outcoupled atoms is analyzed by the same method as the experimental data.

We plot the simulated p_k/v_k (dashed line, in the same units as experiment). The simulation and Beliaev damping theory agree in the regime of experimentation, indicating a window of validity for the assumptions used in analyzing the experimental data. At large k (above $k = 4.09$), t_{eff} is made shorter by the rapid transit of the condensate by the excitations. At low k (less than $k = 1.06$) many of the collisional products remain inside the condensate volume, and are not counted, preventing analysis in this regime.

The arbitrary unit suppression used in Fig. 4 (both for simulation and experiment) was set at $k = 2.63$. The absolute cross-sections obtained by comparing the experimental data to the hydrodynamical simulations were higher than the theoretical values by a k-independent overall factor of 2.36 ± 0.08, which is not understood. This factor may be caused by various inaccuracies in the TOF parameters of the simulation. However, the trend in the experimental analysis is robust, and does not depend on absolute calibration.

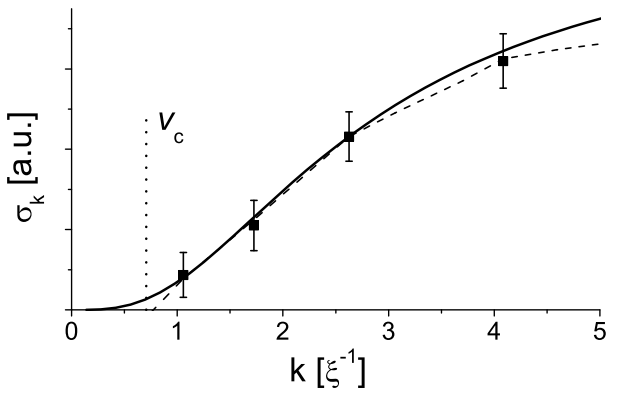

FIG. 4. Suppression of identical particle collisions. Scattering cross-section is in arbitrary units. The momentum is in units of the inverse healing length after LDA averaging, $\xi = 0.24\mu m$. The theoretical curve (solid line) is a LDA average of Eq. (3) [25]. The assumptions of our analysis are tested using hydrodynamic simulations, and found to agree with Beliaev damping theory in the experimental regime (dashed line).

We also set the collision rate artificially to zero in the simulation, and find N_{mom}/N_{count} to be unity within 2%, for all k. This implies that there are no significant other mean-field repulsion effects along the z-axis [22], confirming our assumption of momentum conservation.

In conclusion, we report a measurement of the suppression of the collision cross-section for identical particles within a Bose-Einstein condensate. We find the suppressions in our experiment in agreement with a calculation of Beliaev damping rates, within an overall factor. We use a hydrodynamic simulation of the expansion dynamics, in order to verify our analysis of the experiment. This represents the first measurement of this effect in the quasi-particle continuous spectrum regime.

In the low temperature limit discussed in this Letter, the non-linear coupling mechanism of the interaction Hamiltonian is predicted to generate squeezing and entanglement of quasi-particle excitations [28]. Further experimental study should also lead to an understanding of these processes in the context of the decoherence of excitations and coherent states due to collisional losses within a BEC [29], [30], [31].

This work was supported in part by the Israel Science Foundation and by Minerva foundation.

[1] A.P. Chikkatur et al., Phys. Rev. Lett. **85**, 483 (2000).
[2] M. Modugno et al, Phys. Rev. A **62**, 63607 (2000).
[3] Y.B. Band et al., Phys. Rev. A **64**, 023607 (2001).
[4] R. Onofrio et al., Phys. Rev. Lett. **85**, 2228 (2000).
[5] S. Burger et al., Phys. Rev. Lett. **86**, 4447 (2001).
[6] S. T. Beliaev, Soviet Physics JETP 34(7) **2**, 299 (1958).
[7] L.P. Pitaevskii and S. Stringari, Phys. Lett. A **235**, 398 (1997).
[8] S. Giorgini, Phys. Rev. A **57**, 2949 (1998).
[9] K. Das and T. Bergeman, Phys Rev. A **64**, 013613 (2001).
[10] M. Imamovic-Tomasovic and A. Griffin, Journ. of Low Temperature Physics, **122**, 617 (2001).
[11] W. Ketterle and S. Inouye, Compte rendus de l'academie des sciences, Serie IV - Physique Astrophysique, vol. 2, 339 (2001).
[12] F. Zambelli, et al, Phys. Rev. A **61**, 063608 (2000).
[13] J. Steinhauer, R. Ozeri, N. Katz and N. Davidson, Phys. Rev. Lett. **88**, 120407 (2002).
[14] N. N. Bogoliubov, J. Phys. (USSR) **11**, 23 (1947).
[15] J. M. Vogels et al., Phys. Rev. Lett. **88**, 060402 (2002).
[16] R. P. Feynman, Phys. Rev. **94**, 262 (1954).
[17] L. Deng et al., Nature **398**, 218 (1999).
[18] Y. B. Band, M. Trippenbach, J. P. Burke and P. S. Julienne, Phys. Rev. Lett. **84**, 5462 (2000).
[19] E. Hodby, O. M. Marago, G. Hechenblaidner and C. J. Foot, Phys. Rev. Lett. **86**, 2196 (2001).
[20] T. Esslinger, I. Bloch, and T. W. Hansch , Phys. Rev. A **58**, R2664 (1998).
[21] M. Kozuma et. al., Phys. Rev. Lett. **82**, 871 (1999).
[22] R. Ozeri, J. Steinhauer, N. Katz and N. Davidson, Phys. Rev. Lett. **88**, 220401 (2002).
[23] For $k = 1.06$, there are atoms in front and behind the BEC that should be counted in our integration. We use computerized tomography [22], to find the correct atomic distribution. The systematic error caused by naively integrating the absorption image, can be as large as 10%, which is unacceptable for our purposes. At higher k, these systematic integration effects are verified to be negligible.
[24] hydrodynamical simulations (described below) indicate that there are few higher order multiple collisions for the experimental parameters. We also find that nearly all the collision products are indeed located in the counting region after TOF, confirming our momentum and atom number counting procedures.
[25] The LDA average of the suppression of collisions for an non-homogenous BEC is nearly indistinguishable from the suppression of a homogenous condensate with the LDA average healing length as defined in [13].
[26] F. Dalfovo, S. Giorgini, Lev P. Pitaevskii , S. Stringari, Rev. Mod. Phys. **71**, 463 (1999).
[27] Y. Castin and R. Dum, Phys. Rev. Lett. **77**, 5315 (1996).
[28] J. Rogel-Salazar, G. H C. New, S. Choi and K. Burnett, Phys. Rev. A **65**, 023601 (2002).
[29] T. Nicuni and A. Griffin, e-print cond-mat/0107444v2.
[30] D. S. Jin et. al., Phys. Rev. Lett. **78**, 764 (1997).
[31] F. Ferlaino et. al., e-print cond-mat/0202369.